The Morphological Relationship Between Dome-Shaped Macula and Myopic Retinoschisis: A Cross-sectional Study of 409 Highly Myopic Eyes

Dong Fang, Zhaotian Zhang, Yantao Wei, Li Wang, Ting Zhang, Xintong Jiang, Yunhong Shi, and Shaochong Zhang

State Key Laboratory of Ophthalmology, Zhongshan Ophthalmic Center, Sun Yat-sen University, Guangzhou, People's Republic of China

Correspondence: Shaochong Zhang, State Key Laboratory of Ophthalmology, Zhongshan Ophthalmic Center, Sun Yat-sen University, 54S Xianlie Road, Guangzhou 510060, China; zhangshaochong@gzzoc.com.

DF and ZTZ contributed equally to the work presented here and should, therefore, be considered equivalent authors.

Received: September 7, 2019
Accepted: November 26, 2019
Published: March 16, 2020

Citation: Fang D, Zhang Z, Wei Y, et al. The morphological relationship between dome-shaped macula and myopic retinoschisis: a cross-sectional study of 409 highly myopic eyes. *Invest Ophthalmol Vis Sci.* 2020;61(3):19. https://doi.org/10.1167/iovs.61.3.19

Purpose. The purpose of this study was to analyze the clinical features of dome-shaped macula (DSM) in highly myopic eyes and its morphological relationship with myopic retinoschisis (MRS).

Methods. In this cross-sectional study, 409 eyes of 409 patients with high myopia who had spectral-domain optical coherence tomography (OCT) examinations were included. The associations of DSM with the distribution of MRS and ocular biometry were evaluated.

Results. Of 409 eyes, DSM was detected in 64 eyes (15.6%). The eyes with DSM were more myopic (-18.8 ± 3.9 vs. -13.4 ± 5.9; $P < 0.001$) and had longer axial length (31.7 ± 2.4 vs. 29.5 ± 2.5; $P < 0.001$) compared with those without DSM. A higher rate of extrafoveal retinoschisis (35.9% vs. 9.6%; $P < 0.001$) and a lower rate of foveoschisis (10.9% vs. 26.1%; $P = 0.01$) were detected in the eyes with DSM compared with those without DSM. In the eyes with DSM, MRS was detected in 30 eyes (46.9%). MRS predominantly affected the extrafoveal area (76.7%), especially the base of the dome (82.6%). The extrafoveal retinoschisis was most frequently distributed in the superior quadrant (52.2%). None of the eyes with DSM displayed fovea-only retinoschisis. The ratio of the height and width of the macular bulge was higher in eyes with MRS than those without MRS (0.05 vs. 0.04; $P = 0.001$).

Conclusions. A DSM is found in highly myopic eyes with a longer axial length. MRS in eyes with DSM is more likely to affect the extrafoveal area, especially the base of the dome. A steeper macular bulge is associated with the occurrence of MRS.

Keywords: dome-shaped macula, myopic retinoschisis, high myopia, optical coherence tomography

Dome shaped macula (DSM) was initially described by Gaucher et al.[1] as an inward elevation of the macula within a staphyloma in highly myopic patients as diagnosed by optical coherence tomography (OCT). Although DSM now has been well-characterized by means of OCT, its pathogenesis remains controversial. A higher prevalence of DSM is strongly associated with highly myopic eyes with posterior staphyloma. Thus, hypotheses about its pathogenesis related to high myopia have been proposed: scleral resistance to staphylomatous deformation, adaptive or compensatory response to a myopic ocular expansion.[1,2] DSM has been described in western countries and Japan. Yet, the prevalence of DSM differs among ethnicities, which was reported as 20.1% in Japan[3] and 10.7% to 18% in western countries.[1,4] Similarly, the clinical features of DSM varied in different population.[3–6]

Close associations have been reported between DSM and many maculopathies, including myopic retinoschisis (MRS).[3,7] MRS is one of the main complications leading to visual loss in highly myopic eyes, appeared as splitting or formation of an intraretinal cyst separating the retina with intraretinal columns in OCT. The occurrence of MRS was thought to be associated with vitreomacular traction, the elongation of the eye, and the deformation of the posterior pole eye shape.[7,8] Among them, posterior staphyloma is a typical myopic deformation of the posterior pole eyeball, appeared as a local outpouching of the ocular wall. Previous studies have been mainly concentrated on documenting the relationship between posterior staphyloma and MRS.[9–11] DSM is another type of ocular deformation appearing opposed to a typical posterior staphyloma. However, to the best of our knowledge, little information is available on its association with MRS.

Thus, we sought to evaluate the clinical features of DSM and its morphological relationship with MRS in a large series of highly myopic patients. The features observed were correlated with ocular biometry and other macular complications. By analyzing the distribution features of MRS in eyes with DSM, our goal was to elucidate the potential role of DSM in the pathogenesis of MRS. The possible inter-relationships

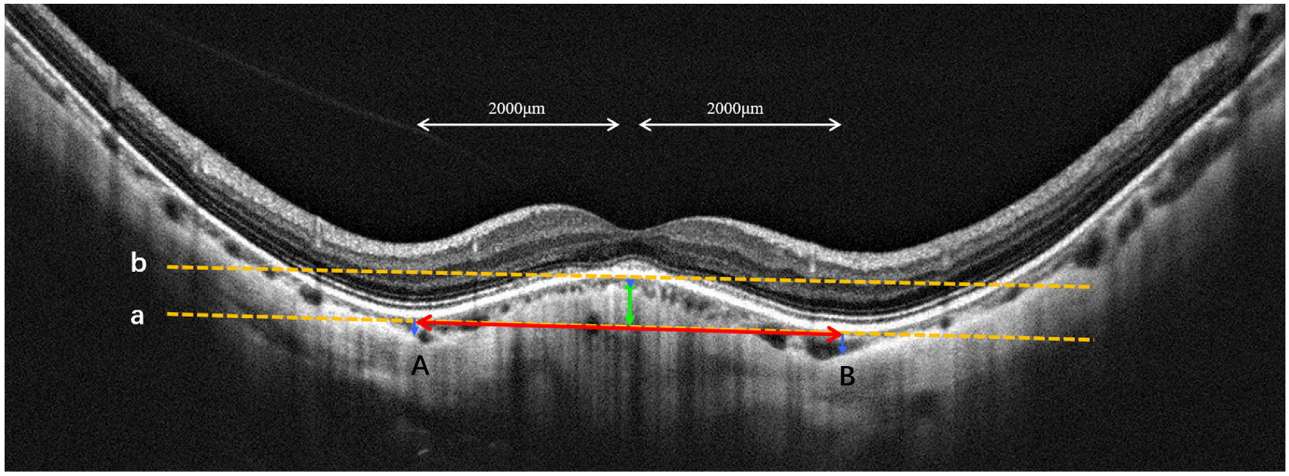

Figure 1. Parameters measured in images of spectral-domain optical coherence tomography in eyes with dome-shaped macular configuration. A dashed yellow line was drawn at the tangent plane at the outer surface of the retinal pigment epithelium (line a). The width of the macular bulge was defined as the distance between the two tangent points (**A**, **B**) in line a (red arrow). An auxiliary line (dashed yellow line) was drawn parallel to line a at the fovea (line b). The distance between line a and line b is equivalent to macular bulge height (green arrow). Choroidal thicknesses were measured at the fovea and the points 2000 μm nasal, temporal, superior, and inferior to the fovea (blue arrow).

between them were also analyzed from a mathematical viewpoint in the current study.

Methods

This study was approved by the institutional research committee of the Zhongshan Ophthalmic Center of Sun Yat-sen University (Guangzhou, China) and was performed in accordance with the World Medical Association's Declaration of Helsinki. The medical records of consecutive patients with high myopia at the Zhongshan Ophthalmic Center between May 2016 and January 2019 were reviewed. Inclusion criteria were (1) highly myopic eyes, defined by refractive error (expressed as spherical equivalent, SE) <-6 diopter (D) or by an axial length ≥26.5 mm; (2) undergone spectral-domain OCT examinations, including vertical scan, horizontal scan, and radial scans through the fovea; (3) complete clinical data including best corrected visual acuity (BCVA), refractive error, axial length, and fundus photographs. Exclusion criteria were (1) eyes with previous vitreoretinal surgery; (2) eyes with any associated or concomitant retinopathy that could confound the retinal interpretation of OCT images; (3) OCT images with poor quality, which was defined as insufficient visualization of the retinal pigment epithelium (RPE) line in the macular area. Only one eye of each participant was used for analysis. When both eyes of the same individuals were included, the right eye was considered for the analysis.

All patients underwent a comprehensive ophthalmological examination, including refractometry using autorefractor (KR-8800; Topcon, Tokyo, Japan), fundus photographs (Visucam; Carl Zeiss Meditec, Jena, Germany), and OCT. The axial length of each participant was measured using IOL Master (Carl Zeiss Meditec). OCT images were obtained with a spectral-domain OCT (Optovue Inc., Fremont, CA, USA) by an experienced examiner. The central wavelength of the OCT device was 840 nm, the scan rate was 26,000 A-scans/s, and the axial resolution was 5 μm. Vertical and horizontal scans, passing through the center of the fovea and radial scans, covering all the macular complications, were obtained in each eye. All data were fully anonymized before access by the researchers.

Two experienced retinal specialists (S.Z. and Y.W.) read all of the OCT images, and agreement by the two specialists was needed to determine the presence of DSM and MRS. Another specialist would be enrolled if there was a disagreement, and diagnosis was provided according to the rule of majority. DSM was defined as an inward bulging of the RPE line with a maximal height >50 μm above a presumed line tangent to the outer surface of the RPE (Fig. 1). The width of the macular bulge was defined as the distance between the two tangent points in the presumed line, and the distance between the peak and the base of the elevation was defined as the height of the macular elevation. The ratio of the height and width (H/W ratio) of the elevation was calculated to evaluate the shape of the macular bulge. Both the bulge height based on the vertical and horizontal sections were measured, and the section showing a bulge >50 μm was used for calculations. For patients who showed a bulge >50 μm in both sections, the average of the vertical and horizontal measurement was used for analysis. The choroidal thickness (CT) was defined as the distance from the RPE line to the inner surface of the sclera using a masked author. CT was measured at the fovea and at 4 parafoveal locations 2000 μm from the foveal center with a built-in caliber tool within the software. Because the magnification of the OCT image was affected by the axial length variation, the measured distance was corrected by using the method described by Sampson et al.[12] CT at the fovea was calculated as the average of the measurements in the vertical and horizontal OCT images.

The incidence of DSM, the distribution features of retinoschisis in eyes with and without DSM, and the associations between DSM and MRS were analyzed. The outer retinoschisis was graded according to the location and the size, as suggested by Shimada et al.[13]: no macular retinoschisis (S0); extrafoveal macular retinoschisis (S1); fovea-only macular retinoschisis (S2); foveal but not the entire macular area macular retinoschisis (S3); and the entire macular area macular retinoschisis (S4). Other macular complications,

Investigative Ophthalmology & Visual Science

Table 1. Comparison of Clinical Characteristics of Eyes With and Without Dome-shaped Macula

Characteristics	Dome-shaped Macula		*P* value
	Present	Absent	
No. of eyes (patients)	64 (64)	345 (345)	
Men (%)	29 (45.3)	157 (45.5)	1.0*
Women (%)	35 (54.7)	188 (54.5)	
Age, y			0.60†
Mean ± SD	49.37 ± 13.76	47.15 ± 16.90	
Range	23–78	4–84	
BCVA (logMAR)			0.91†
Mean ± SD	0.71 ± 0.51	0.78 ± 0.65	
Range	0.05–1.85	-0.08 to -2.6	
Refractive error, D			**<0.001**†
Mean ± SD	−18.8 ± 3.9	−13.4 ± 5.9	
Range	−9 to −29	−5 to −39	
Axial length, mm			**<0.001**†
Mean ± SD	31.7 ± 2.4	29.5 ± 2.5	
Range	26.3–37.4	24.9–38	
Macular complication			
FS, n (%)	7 (10.9)	90 (26.1)	**0.01**‡
EFRS, n (%)	23 (35.9)	33 (9.6)	**<0.001**‡
CNV (%)	3 (4.7)	15 (4.3)	1.00§
Serous RD (%)	1 (1.6)	0	0.16§
LMH (%)	7 (10.9)	24 (7.0)	0.30‡
Outer lamellar macular hole (%)	0	27 (6.6)	**0.01**§
FTMH (%)	1 (3.2)	17 (4.6)	0.33§
Tractional lesions (%)	30 (46.9)	127 (36.8)	0.13§
ERM	17	88	
VA	8	8	
VT	5	34	

D, diopters; logMAR, logarithm of the minimum angle of resolution; FS, foveal retinoschisis; EFRS, extrafoveal retinoschisis; RD, retinal detachment; LMH, lamellar macular hole; ERM, epiretinal membrane; VA = vitreomacular adhesion; VT = vitreomacular traction.

Statistically significant *P* values were reported in bold.

* *t*-tests.

† Mann-Whitney *U* test.

‡ χ^2 tests.

§ Fisher's exact tests.

including serous retinal detachment, epiretinal membrane, full thickness macular hole, lamellar macular hole, outer lamellar macular hole, and choroidal neovascularization were also analyzed. All cases of choroidal neovascularization (CNV) were diagnosed through a combination of OCT and fundus fluorescein angiography.

Age, refractive error, axial length, BCVA, CT, the H/W ratio of the macular bulge were compared between the eyes with and without DSM using independent sample *t*-tests or Mann-Whitney *U* tests. The incidences of various macular complications between the eyes with and without DSM were compared using χ^2 tests or Fisher exact probability tests. The comparisons of CT measurements were adjusted for multiple comparisons by using Bonferroni test. Multivariate binary regression analysis was performed with the presence of DSM as the dependent variable, and age, axial length, the pattern of MRS (categorical variable: eyes without MRS were set as 1, extrafoveal retinoschisis as 2, and foveal retinoschisis as 3) as independent variables. For the eyes with DSM, multivariable binary regression analysis was also performed with the presence of MRS as the dependent variable, and age, axial length, the presence of tractional lesions, and H/W ratio of the macular bulge as independent variables. A P value of < 0.05 was considered statistically significant. All data was analyzed using the SPSS 19.0 statistical software (SPSS Inc., Chicago, IL, USA).

Results

A total of 409 eyes of 409 consecutive patients with high myopia who underwent OCT imaging were studied. In the image interpretation, the two ophthalmologists yielded a consistent rate of 100% on the diagnosis of the DSM, and a consistent rate of 98.0% (401/409 eyes) on the diagnosis of the MRS. Eight eyes with disagreement on diagnosis were re-examined by the third ophthalmologists to draw the final diagnosis according to the rule of majority. The objects comprised 223 women and 186 men with a mean age of 47.5 years ranging from 4 to 84 years old. The mean refractive error was −14.5 D with a range of −5 to −39.0 D. The mean axial length was 29.9 mm with a range of 24.9 to 38.0 mm.

Clinical Characteristics of Eyes with Dome-Shaped Macula

Among the 409 eyes, 64 eyes (15.6%; 64 patients) had a DSM. The DSM was bilateral in 22 patients and unilateral in 42 patients. No significant differences were observed based on age between patients with unilateral involvement and bilateral involvement (48.57 ± 14.02 vs. 51.00 ± 13.21; $P = 0.60$). OCT images of the posterior pole showed that there were 3 patterns of DSM: 48 horizontal oval-shaped DSM, 5 vertical oval-shaped DSM, and 7 DSM with a round dome. The

Investigative Ophthalmology & Visual Science

clinical characteristics of 64 eyes with DSM and 345 eyes without DSM were summarized in Table 1. Statistical comparison between the eyes with and without DSM showed that patients with DSM were more myopic (−18.8 ± 3.9 vs. −13.4 ± 5.9 D; $P < 0.001$) and had longer axial length (31.7 ± 2.4 vs. 29.5 ± 2.5 mm; $P < 0.001$) compared with those without DSM. However, there was no significant difference in BCVA between them (0.71 ± 0.51 vs. 0.78 ± 0.65; $P = 0.91$). Between eyes with and without DSM, comparisons were made of the incidence of the macular lesions (Table 1). Extrafoveal retinoschisis were observed more frequently in eyes with DSM than in those without DSM (23/64 [35.9%] vs. 33/345 [9.6%]; $P < 0.001$). By contrast, foveoschisis were detected less frequently in eyes with DSM than in those without DSM (7/64 [10.9%] vs. 90/345 [26.1%]; $P = 0.01$). The proportion of outer lamellar macular hole (0 vs. 6.6%; $P = 0.01$) was evidently lower in eyes with DSM. The differences of the proportion of serous retinal detachment, lamellar macular hole, and full-thickness macular hole were not significant between the eyes with and without DSM ($P = 0.16$; $P = 0.30$; and $P = 0.33$). Subgroup comparison between the young (age <=50 years) and the old (age >50 years) individuals was also been conducted. The results showed that the older patients had longer axial length and worse vision with higher prevalence of MRS compared with the younger patients. However, no significant difference was found on the prevalence of DSM between the young and the old (see Supplementary Table S1).

Clinical Characteristics of Eyes With Dome-Shaped Macula and Myopic Retinoschisis

Among the eyes with DSM, further comparison was made between the eyes with and without MRS (Table 2). Among the eyes with DSM, 30 eyes were with MRS and 29 eyes were without MRS (because foveoschisis might be sheltered by the presence of full-thickness macular hole (FTMH), serous retinal detachment (SRD), or CNV, therefore, eyes with these macular complications were excluded in this subgroup analysis). The results showed that the patients with DSM and MRS were obviously older (54.7 ± 12.5 vs. 45.9 ± 13.6; $P = 0.01$) and had worse vision (0.78 ± 0.47 vs. 0.50 ± 0.34; $P = 0.02$) compared with the patients without MRS. The differences were not significant in SE ($P = 0.09$) and in axial length ($P = 0.91$) between the eyes with and without MRS. The H/W ratio of the macular elevation was used to evaluate the shape of the macular bulge. A higher H/W ratio indicates a steeper macular bulge, whereas a lower H/W ratio denotes a flatter bulge. Subgroup analysis showed that the eyes with DSM and MRS had a higher H/W ratio, which reveals a steeper bulge compared with the eyes without MRS (0.05 ± 0.01 vs. 0.04 ± 0.01; $P = 0.001$). No significant differences were found on the subfoveal and parafoveal CT between the eyes with and without MRS ($P = 0.73$; $P = 0.44$; $P = 0.32$; $P = 1.00$; and $P = 0.10$).

The Distribution Features of Retinoschisis in the Eyes With DSM

An MRS was detected in 159 eyes among the highly myopic eyes (38.9%). Thirty eyes were with DSM and 129 eyes were without DSM. In 30 eyes with MRS and DSM, inner retinoschisis was observed in 19 eyes (63.3%), and all eyes with inner retinoschisis showed concomitant outer retinoschisis. Twenty-three eyes (76.7%) exhibited grade S1 outer retinoschisis, none of the eyes displayed retinoschisis limited to the foveal region (grade S2 outer retinoschisis), four eyes (13.3%) showed grade S3 outer retinoschisis, and three eyes (10.0%) had grade S4 outer retinoschisis (Table 3). Twenty-three eyes showed S1 outer retinoschisis, a typical fovea-sparing outer retinoschisis was noted in eyes with DSM, which shows the outer retinoschisis affecting the entire macular region except for the foveal region in the center of the DSM (Fig. 2 first row). The extrafoveal retinoschisis in eyes with DSM was more likely to affect the superior quadrant (52.2%), followed by the inferior quadrant (47.8%), nasal quadrant (39.1%), and temporal quadrant (30.4%; Fig. 3). In addition, the extrafoveal retinoschisis was more likely to affect the base of the dome (19/23; 82.6%; Fig. 2 second row, Fig. 4). For seven eyes showing foveoschisis (S3, S4), tractional lesions were found at the fovea in all eyes (7/7; 100%; Fig. 2 third and fourth row). The incidence of tractional lesions was higher in the eyes with foveoschisis than in those with extrafoveal retinoschisis

Table 2. Comparison of Clinical Characteristics Between Eyes With and Without Myopic Macular Retinoschisis Among the Eyes With Dome-Shaped Macula

Characteristics	Myopic Macular Retinoschisis		*P* value
	Present	Absent	
No. of eyes	30	29	
Age, y			**0.01**[*]
Mean ± SD	54.7 ± 12.5	45.9 ± 13.6	
Range	23–78	28–75	
BCVA (logMAR)			**0.02**[†]
Mean ± SD	0.78 ± 0.47	0.50 ± 0.34	
Range	0.10–1.70	0.05–1.30	
Refractive error, D			0.09[*]
Mean ± SD	−19.8 ± 4.1	−18.0 ± 3.7	
Range	−9 to −29	−9.5 to −26.5	
Axial length, mm			0.91[*]
Mean ± SD	31.7 ± 1.9	31.6 ± 3.0	
Range	27.2–35.6	26.3–37.4	
DSM height			0.27[*]
Mean ± SD	121.2 ± 47.9	107.4 ± 46.9	
Range	51–253	51–205	
DSM H/W Ratio			**0.001**[*]
Mean ± SD	0.05 ± 0.01	0.04 ± 0.01	
Range	0.03–0.07	0.04–0.06	
CT			
Subfoveal CT	33.2 ± 24.4	52.8 ± 52.8	0.73[‡]
Superior CT	30.9 ± 16.2	54.6 ± 42.4	0.44[‡]
Inferior CT	26.0 ± 15.3	50.8 ± 45.0	0.32[‡]
Nasal CT	26.8 ± 15.5	37.1 ± 25.6	1.00[‡]
Temporal CT	29.5 ± 19.7	57.6 ± 54.2	0.10[‡]
Tractional lesions (%)	17 (56.7)	12 (41.4)	0.3[§]
ERM	12	5	
VA	2	5	
VT	3	2	

D = diopters; logMAR = logarithm of the minimum angle of resolution; ERM = epiretinal membrane; VA = vitreomacular adhesion; VT = vitreomacular traction.

Statistically significant *P* values were reported in bold.

[*] *t*-tests.

[†] Mann-Whitney *U* test.

[‡] *P* values were adjusted for multiple comparisons using the Bonferroni test.

[§] Fisher's exact tests.

Investigative Ophthalmology & Visual Science

Table 3. The Spatial Distribution of Macular Retinoschisis in Eyes With and Without Dome-Shaped Macula

Characteristics	Dome-shaped Macula		P value
	Present	Absent	
No. of eyes (patients)	30 (30)	129 (129)	
Outer RS*, n (%)	30 (100)	123 (95.3)	
Grade			**<0.001**†
S1 (%)	23 (76.7)	33 (26.8)	
Location of RS			
Superior (%)	12 (52.2)	9 (27.3)	
Inferior (%)	11 (47.8)	25 (75.8)	
Nasal (%)	9 (39.1)	10 (30.3)	
Temporal (%)	7 (30.4)	7 (21.2)	
S2 (%)	0	16 (13.0)	
S3 (%)	4 (13.3)	28 (22.8)	
S4 (%)	3 (10.0)	46 (37.4)	

RS, retinoschisis.
Statistically significant *P* values were reported in bold.
* Eyes with concomitant inner retinoschisis were included.
† Fisher's exact tests.

(100% vs. 43.5%; $P = 0.01$). The distribution of different lesions was listed as follows: epiretinal membrane, 42.9% (3 of 7 eyes) with a foveoschisis and 39.1% (9 of 23 eyes) with an extrafoveal retinoschisis; vitreomacular traction, 42.9% (3 of 7 eyes) versus 0 (0 of 23 eyes); and vitreomacular adhesion, 14.2% (1 of 7 eyes) versus 4.3% (1 of 23 eyes).

The Distribution Features of Retinoschisis in the Eyes Without DSM

In contrast, retinoschisis in eyes without DSM showed a different spatial distribution (Table 3). In 129 eyes with MRS without DSM, 6 eyes had only an inner retinoschisis, 63 eyes had both an outer and inner retinoschisis, and 60 eyes had only an outer retinoschisis. In 123 eyes with outer retinoschisis, 33 eyes (26.8%) exhibited grade S1 outer retinoschisis, 16 eyes (13.0%) displayed grade S2 outer retinoschisis, 28 eyes (22.8%) showed grade S3 outer retinoschisis, and 46 eyes (37.4%) showed grade S4 outer retinoschisis (Table 3). In addition, extrafoveal retinoschisis in eyes without DSM was more likely to affect the inferior (75.8%) quadrant before affecting the nasal (30.3%), superior (27.3%), and temporal quadrant (21.2%; Fig. 3).

Multivariate binary analysis adjusted for age and axial length to specifically evaluate the contribution of MRS to the presence of DSM revealed that DSM had significant correlation with the pattern of MRS ($P = 0.01$; odds ratio, 0.56; 95% confidence interval, 0.37−0.87), and axial length ($P < 0.001$; odds ratio, 2.07; 95% confidence interval, 1.70−2.53).

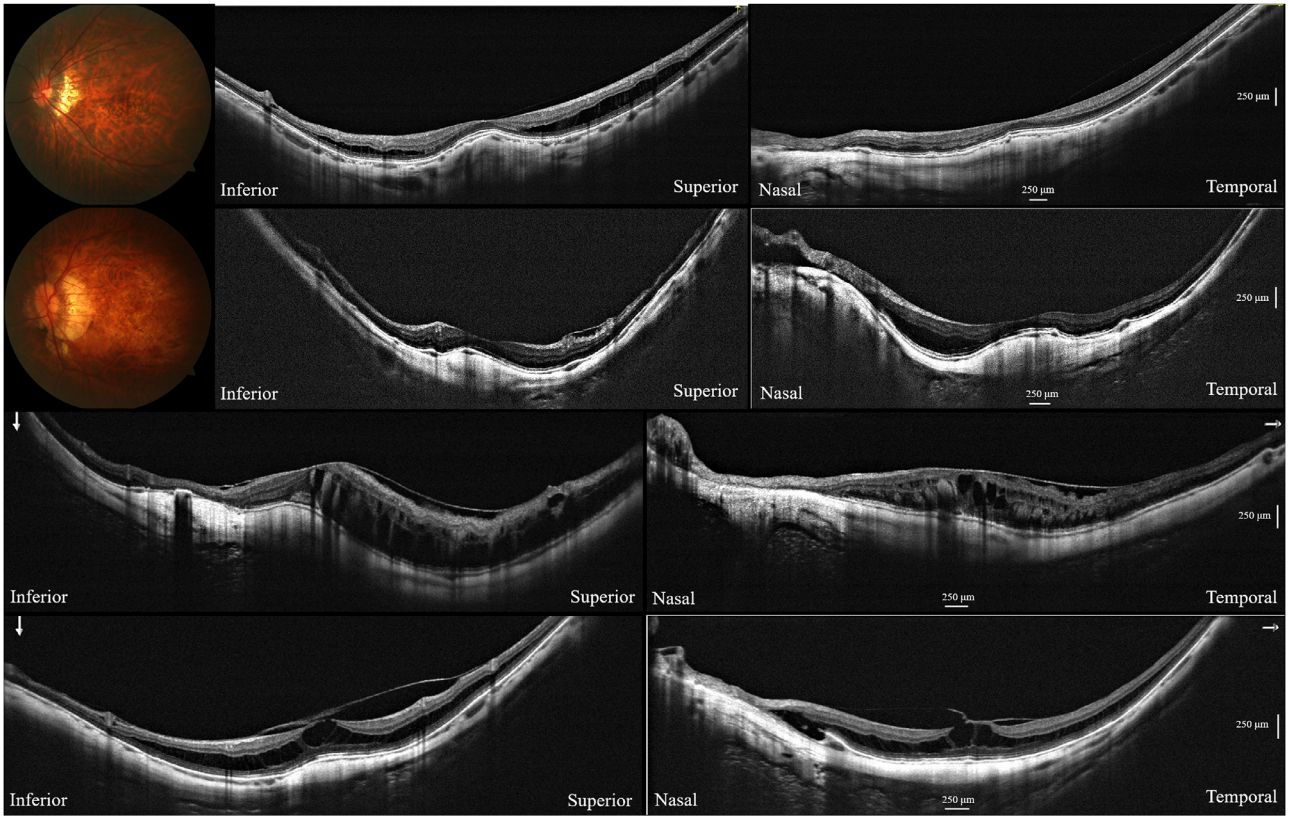

Figure 2. Eyes with high myopia showed DSM within the posterior staphyloma. (Top row) Fundus photograph and OCT of a 42-year-old woman. (Top middle) The vertical OCT scan show an inward convexity of the RPE within the staphyloma. A representative fovea-sparing outer retinoschisis, which means the outer retinoschisis affecting the entire macular region except for the foveal region in the center of the DSM was noted. (Top right) The horizontal scan shows an almost flat contour of the RPE. (Second row) Fundus photograph and OCT of a 62-year-old woman. The vertical OCT scan exhibits a slightly inward convexity (<50 μm) of the RPE. The horizontal scan displays an obvious inward convexity of the RPE within the staphyloma, and outer retinoschisis affecting the nasal base of DSM and peripapillary area. (Third and fourth rows) Foveoschisis in highly myopic eyes with DSM and tractional epiretinal membrane. Tractional epiretinal membrane at the fovea with foveoschisis (third row) and lamellar hole (fourth row) in eyes with horizontal oval-shaped DSM.

Investigative Ophthalmology & Visual Science

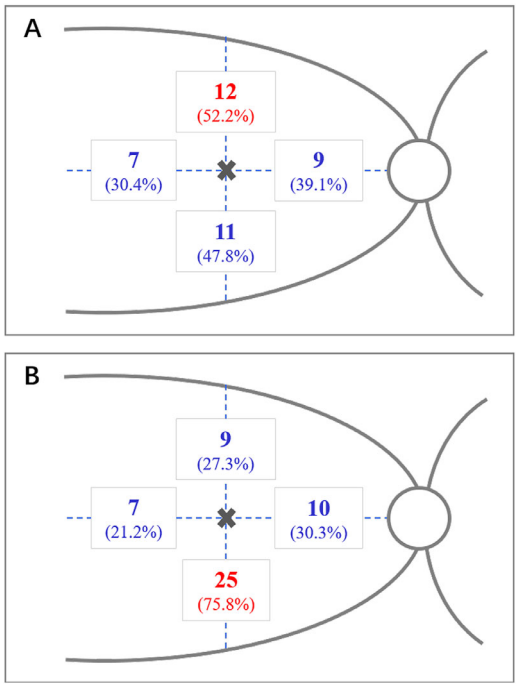

Figure 3. The spatial distribution of outer extrafoveal retinoschisis in eyes with DSM (**A**) and eyes without DSM (**B**) in schematic diagrams. The superior quadrant has the highest proportion (52.2%) of extrafoveal retinoschisis in the highly myopic eyes with DSM (**A**), whereas the inferior quadrant has the highest proportion (75.8%) of extrafoveal retinoschisis in the eyes without DSM (**B**). Both cases consistently show the lowest proportion affecting the temporal quadrant.

For the eyes with DSM, multivariate binary analysis with the presence of MRS as the dependent variable revealed that a higher prevalence of MRS was associated with a higher H/W ratio ($P = 0.01$; odds ratio, 4.12; 95% confidence interval, 2.12−8.00).

Discussion

The results of group comparisons showed that MRS in eyes with DSM predominantly affected the extrafoveal area, especially the base of the dome. Eyes with MRS showed a steeper macular bulge compared with the eyes without MRS. This is consistent with the results of multiple regression analysis, which revealed that the prevalence of DSM was associated predominantly with the pattern of MRS, and that the prevalence of MRS was associated with the shape of the macular bulge. To our best knowledge, the present study first provided a detailed description of the distribution and extent of MRS in eyes with DSM, and to connect it with the shape of the macular bulge.

The incidence rate of DSM was 15.6% (64/409) in highly myopic eyes in our study, which was comparable with the rate of 13.8% (123 of 891 highly myopic cataract eyes) reported in another study in Chinese patients[14] and of 10.7% (28 of 260 highly myopic eyes) reported in a European population.[15] Our reported rate was lower than that reported by Liang et al.[3] in a Japanese group (225/1118; 20.1%). The differences might result from the different inclusion criteria among studies. In Liang's study, the SE was ≤−8.0 D or axial length of ≥26.5 mm, which resulted in a more myopic population. For eyes with DSM, no significant differences based on age was detected between patients with unilateral involvement and bilateral involvement. This was consistent with the previous publications.[1]

In our study, the highly myopic eyes with DSM had greater degree of myopia, longer axial length, and equal BCVA compared with the eyes without DSM. Similarly, Liang et al.[3] found that the highly myopic patients with DSM were more myopic, had longer axial length, and better vision compared with those without DSM. This suggested that DSM might be a protective factor for visual function in extensively elongated myopic eyeballs. In addition, the lower rate of vision-threatening macular complications, such as foveoschisis in eyes with DSM, might partly explain the protective effect.

In the current study, the rate of extrafoveal retinoschisis was higher in eyes with DSM than in eyes without

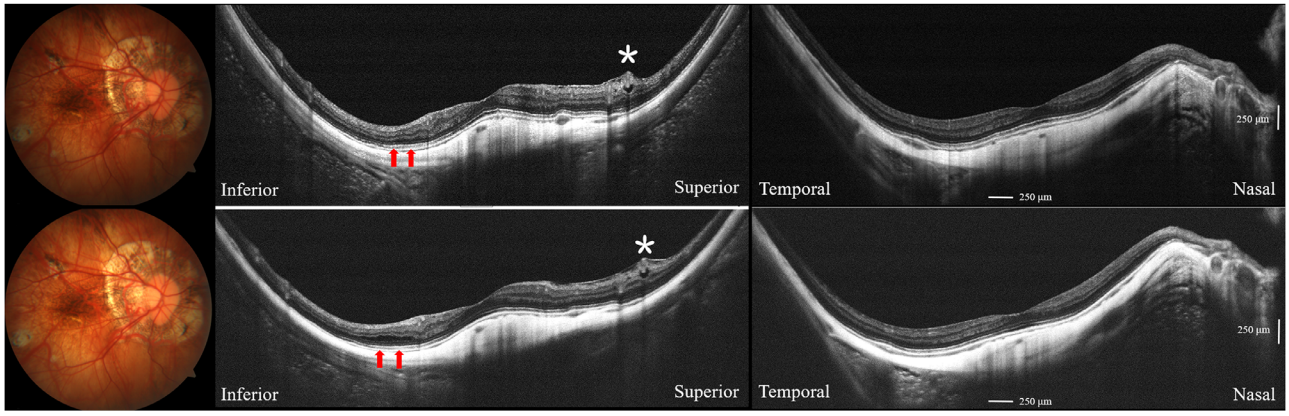

Figure 4. Longitudinal changes in the pattern of extrafoveal retinoschisis in dome-shaped macular configuration. The right eye of a 32-year-old man with high myopia (best corrected visual acuity [logMAR: 0.30], axial length [30.23 mm], and refractive error [−19.5 diopters]). (Upper row) Fundus photograph and OCT at the initial examination. Vertical-scan OCT image shows a dome-shaped macular configuration. Vascular microfold (asterisk) at the superior quadrant was noted, and no obvious outer retinoschisis was noted. (Bottom row) At the end of the follow-up (20 months later), fundus photograph shows no obvious progression of the atrophic changes. A newly developed lesion of extrafoveal retinoschisis was detected at the inferior base of the dome as compared to the initial examination (red arrows). The horizontal scans displayed no obvious progression with time.

Investigative Ophthalmology & Visual Science

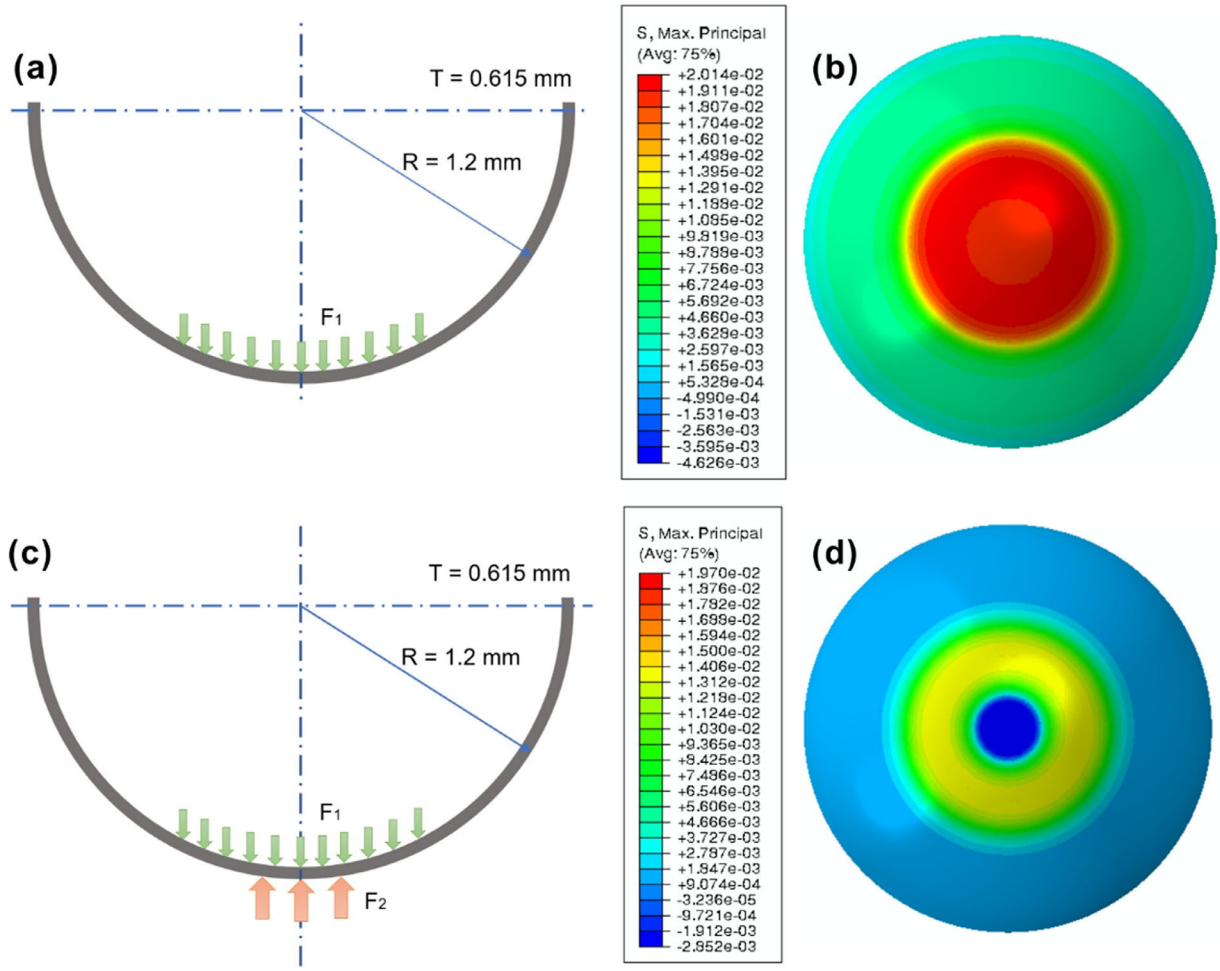

Figure 5. (**A**, **-B**) Geometrical model of the posterior ocular wall with applied pressure F_1 (2 mN) and its corresponding stress distribution (top view), the maximum stress position is located in the center (red circle). (**C**, **D**) Geometrical model of the posterior ocular with applied pressures F_1 (2 mN) and F_2 (4 mN) and its corresponding stress distribution (top view), the maximum stress position is relocated in the peripheral area, where the pressures F_1 and F_2 intersect with each other (yellow ring).

DSM, whereas the rate of foveoschisis shows the opposite. The retinoschisis in eyes with DSM were more likely to affect the extrafoveal area, especially the base of the dome. To better understand the force loading status of the ocular wall under the condition of DSM, we set up a model to simulate the deformation and the forces of the posterior ocular wall. As shown in Figure 5A, a simulation model of the ocular wall was established in a commercial software ABAQUS/Standard. To simplify the simulation process, only the posterior half of the ocular wall was taken into consideration in our model. Pressures were applied to induce deformation of the ocular wall. The material parameters of the retina were referred from published studies[16,17] (Young modulus: 0.2985 Mpa; Poisson ratio: 0.4). With the applied pressure F_1 (see Fig. 5A), the posterior wall deforms outward, evidently simulating the posterior scleral staphyloma condition, and no inward elevation in the posterior pole is observed. Under such loading conditions, the maximum stress position is located in the center from the top view shown in Figure 5B, indicating the central fovea as the weakest point. The stress distributions match well with the higher rate of foveoschisis observed in the condition of posterior staphyloma without DSM.

In another situation, when both outward and inward pressures F_1 and F_2 are applied (see Fig. 5C), an inward elevation occurs in the center within the existing outpouching, which coincides well with the DSM phenomenon. Intriguingly, a switch from tensile stress to compressive stress at the central fovea is observed, and with compressive stress, the central fovea is well protected and is more resilient upon deformation. In addition, it is noted that the maximum stress position moves from the original central position to peripheral area shown in Figure 5D, where the pressure F_1 and F_2 intersect with each other. Therefore, the central fovea is no longer the weakest position, whereas the most vulnerable point is relocated in the stress-concentration position, denoted by a yellow ring in Figure 5D (the same position of the extrafoveal retinoschisis in our experimental observations). The simulation results corresponded well with the morphological relationship between DSM and MRS.

Furthermore, eyes with MRS showed a steeper macular bulge compared with the eyes without MRS. It might suggest that the occurrence of MRS in eyes with DSM was related to a steeper macular elevation, whereas a gentle elevation may be characteristic for eyes without MRS. Thus, the

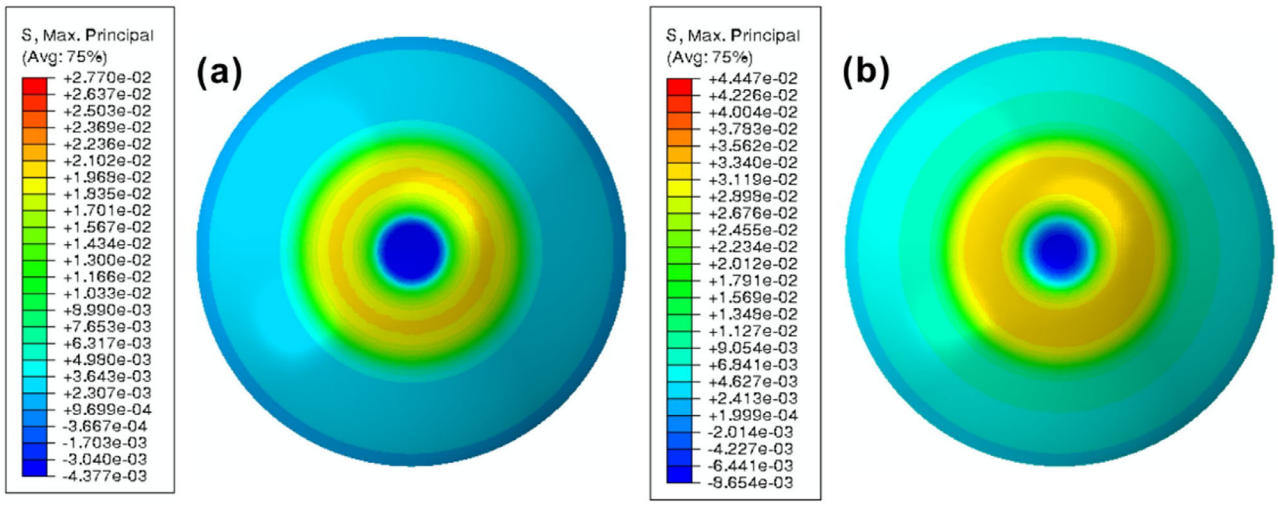

Figure 6. Stress distributions of the posterior ocular with different applied pressures: (**A**) $F_1 = 5$ mN, $F_2 = 10$ mN; (**B**) $F_1 = 10$ mN, $F_2 = 20$ mN, as shown in Figure 5C. With the pressures F_1 and F_2 increased, simulating a steeper DSM condition, the stress concentration positions are almost located in the same area as the one in Figure 5D. In addition, the stress values increase with the increased applied pressures, implying higher possibility of retinoschisis in real eyes.

variations of the stress distributions on the ocular wall were investigated upon increased applied pressures, which are shown in Figure 6. With the pressures F_1 and F_2 increased, simulating a steeper DSM condition, the stress concentration positions are almost located in the same area as the one in Figure 5D. The difference lies in the stress values, which increase obviously with the increased applied pressures as expected. Because the yield and crack processes are not considered in our model, only larger deformation is observed when larger pressures are applied. However, the posterior ocular wall may split in the real world under overload, considering the limited elasticity of the retina. This is partly supported by the data provided by Xu et al.[18] In Xu et al.'s study, younger patients with a more broad and gentle macular elevation presented an evidently lower rate of myopic traction maculopathy, whereas older patients with a steeper macular elevation showed a higher rate of myopic traction maculopathy. However, the current model was a possible mechanism behind the pattern of MRS in DSM based on the precondition that DSM formed earlier than MRS. Further investigations on DSM with long-term follow-up are necessary to validate this theory.

As mentioned above, retinoschisis was less detected at the fovea in the eyes with DSM. There are only seven cases of foveoschisis in the highly myopic eyes with DSM (10.9%). In these eyes, lesions causing an inward traction of the retina were observed evidently frequently (100% vs. 43.5%; $P = 0.01$). This suggested that the mechanisms for causing MRS are probably diverse and complex, and that inward tractional forces at the fovea may play an important role in the development of foveoschisis in eyes with DSM.

This study has several limitations. Given the cross-sectional design of the current study, no data evaluating the dynamic change of DSM and MRS were available. Future studies should be designed to assess whether this morphological association holds after long-term follow-up. Second, the current study was focused on the morphological relationship between DSM and MRS. Functional outcomes were less involved. Further investigations with functional parameters would be demanded.

In summary, this preliminary study demonstrated that highly myopic eyes with DSM were found in eyes with higher degree of myopia and longer axial length. MRS in eyes with DSM was more likely to affect the extrafoveal area, especially the base of the dome. In addition, a steeper macular bulge was correlated to the occurrence of MRS. By providing more information about the severity of the pathological change, namely the distribution and the extent of MRS, the shape of the macular bulge, and analyzing the possible interplay between these two pathological changes by statistical methods and mathematical modeling, we believe our study will provide references for further research and contribute to a better understanding of the mechanism of DSM.

Acknowledgments

The authors thank Wei Wang and Shudong Yu from South China University of Technology for their simulation contributions in this work.

Supported by the Science and Technology Program of Guangzhou (Grant No. 201803010022). The funding organization had no role in the design or conduct of the research.

Disclosure: **D. Fang,** None; **Z. Zhang,** None; **Y. Wei,** None; **L. Wang,** None; **T. Zhang,** None; **X. Jiang,** None; **Y. Shi,** None; **S. Zhang,** None

References

1. Gaucher D, Erginay A, Lecleire-Collet A, et al. Dome-shaped macula in eyes with myopic posterior staphyloma. *Am J Ophthalmol*. 2008;145:909–914.
2. Ohsugi H, Ikuno Y, Oshima K, Yamauchi T, Tabuchi H. Morphologic characteristics of macular complications of a dome-shaped macula determined by swept-source optical coherence tomography. *Am J Ophthalmol*. 2014;158:162–170.e161.
3. Liang IC, Shimada N, Tanaka Y, et al. Comparison of clinical features in highly myopic eyes with and with-

out a dome-shaped macula. *Ophthalmology*. 2015;122:1591–1600.
4. Ceklic L, Wolf-Schnurrbusch U, Gekkieva M, Wolf S. Visual acuity outcome in RADIANCE study patients with dome-shaped macular features. *Ophthalmology*. 2014;121:2288–2289.
5. Zhao X, Ding X, Lyu C, et al. Observational study of clinical characteristics of dome-shaped macula in Chinese Han with high myopia at Zhongshan Ophthalmic Centre. *BMJ Open*. 2018;8:e021887.
6. Errera MH, Michaelides M, Keane PA, et al. The extended clinical phenotype of dome-shaped macula. *Graefes Arch Clin Exp Ophthalmol*. 2014;252:499–508.
7. Wakazono T, Yamashiro K, Miyake M, et al. Association between eye shape and myopic traction maculopathy in high myopia. *Ophthalmology*. 2016;123:919–921.
8. Gohil R, Sivaprasad S, Han LT, Mathew R, Kiousis G, Yang Y. Myopic foveoschisis: a clinical review. *Eye (Lond)*. 2015;29:593–601.
9. Wu PC, Chen YJ, Chen YH, et al. Factors associated with foveoschisis and foveal detachment without macular hole in high myopia. *Eye (Lond)*. 2009;23:356–361.
10. Alkabes M, Pichi F, Nucci P, et al. Anatomical and visual outcomes in high myopic macular hole (HM-MH) without retinal detachment: A review. *Graefes Arch Clin Exp Ophthalmol*. 2014;252:191–199.
11. Shinohara K, Tanaka N, Jonas JB, et al. Ultrawide-field OCT to investigate relationships between myopic macular retinoschisis and posterior staphyloma. *Ophthalmology*. 2018;125:1575–1586.
12. Sampson DM, Gong P, An D, et al. Axial length variation impacts on superficial retinal vessel density and foveal avascular zone area measurements using optical coherence tomography angiography. *Invest Ophthalmol Vis Sci*. 2017;58(7):3065–3072.
13. Shimada N, Tanaka Y, Tokoro T, Ohno-Matsui K. Natural course of myopic traction maculopathy and factors associated with progression or resolution. *Am J Ophthalmol*. 2013;156:948–957.e941.
14. Zhu X, He W, Zhang S, Rong X, Fan Q, Lu Y. Dome-shaped macula: A potential protective factor for visual acuity after cataract surgery in patients with high myopia. *Br J Ophthalmol*. 2019;103:1566–1570.
15. Garcia-Ben A, Kamal-Salah R, Garcia-Basterra I, Gonzalez Gomez A, Morillo Sanchez MJ, Garcia-Campos JM. Two- and three-dimensional topographic analysis of pathologically myopic eyes with dome-shaped macula and inferior staphyloma by spectral domain optical coherence tomography. *Graefes Arch Clin Exp Ophthalmol*. 2017;255:903–912.
16. Sigal IA, Flanagan JG, Ethier CR. Factors influencing optic nerve head biomechanics. *Invest Ophthalmol Vis Sci*. 2005;46(11):4189–4199.
17. Aloy MA, Adsuara JE, Cerda-Duran P, et al. Estimation of the mechanical properties of the eye through the study of its vibrational modes. *PLoS One*. 2017;12:e0183892.
18. Xu X, Fang Y, Jonas JB, et al. Ridge-shaped macula in young myopic patients and its differentiation from typical dome-shaped macula in elderly myopic patients. *Retina*. 2020;40:225–232.